# Supplementary Material (1)

## EAP spatial attenuation reanalyzed in published data

## to

# Dipole Characterization Of Single Neurons From Their Extracellular Action Potentials

Ferenc Mechler and Jonathan Victor

Department of Neurology and Neuroscience,
Medical College of Cornell University, New York, NY

Address for correspondence:
Ferenc Mechler
Department of Neurology and Neuroscience
Medical College of Cornell University
1300 York Avenue, New York, NY 10065-4805
phone: (212) 746-6520
Fax: (212) 746-8984
e-mail: fmechler@med.cornell.edu

## Summary

Here we review and re-analyze the available evidence on the form of spatial attenuation of the extracellular action potential (EAP) of single neurons. We consider modeling studies aimed at revealing basic principles of biophysics [1, 2], numerical simulations aimed at reproducing the details of action potentials in realistic neuron models [3-8], and experimental investigations [9, 10]. The studies reviewed here all focused on pyramidal neurons, some in cat neocortex [2, 4, 5], others in rodent hippocampus [3, 6-10].

Where it was possible, we re-analyzed the published data to make explicit the spatial decay of the EAP amplitude with distance measured from the soma. We have found that the model studies all agreed on two things. (i) Within the immediate neighborhood of the soma ($r<r_0$), spatial attenuation is slower than predicted by a dipole and may or may not be well fit by a monopole model. (ii) The extracellular potential is well approximated by a power function that characterizes the dipole (exponent $k_{\text{model}} = 2$) in the ($r_0 \le r \le 200\mu\text{m}$) range. Essentially, these two observations summarize the EAP signature of the distributed nature of the current sources of real neurons.

The inner limit of the dipole range varies, $r_0 \in [20, 50]\mu\text{m}$, and it depends on cell size and membrane properties: $r_0$ was larger in models of pyramidal cells in cat layer 5 ($r_0 \sim 50\mu\text{m}$) than in the 30-50% smaller rodent CA1 cells ($r_0 \sim 30-40\mu\text{m}$), and larger in models where dendrites not just the soma compartment was endowed with active membrane conductances (probably because this made current sources more spread out). The available experimental data were taken in small samples and the evidence is inconclusive on the rate of the spatial attenuation of the extracellular potential. Each study is discussed separately in more detail below.

## (1) Rall (1962) – a computational study

In this historic paper [1], the earliest study relevant to this issue, Rall analyzed a neuron with a simplified, symmetric, and sparse dendritic arbor and passive membrane properties. He plotted analytic and simulated EAP amplitudes as a function of distance ($r$, measured in multiples of $R$, the soma radius) from the soma in a direction perpendicular to the cell axis (his Figure 10). We re-analyzed his result in Figure 1 below.

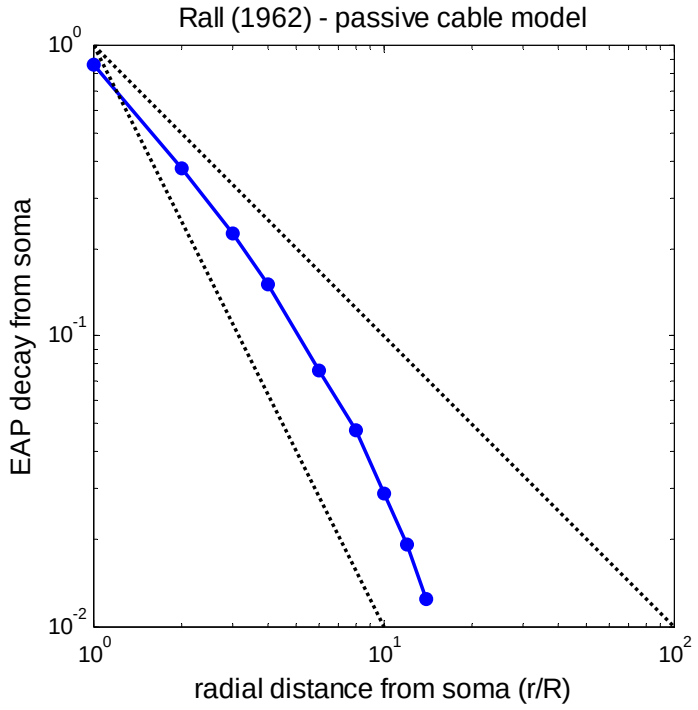


**Figure 1**

Data from [1], i.e., curve F of his Figure 10, are re-plotted here in log-log coordinates (blue symbols). For visual comparison, the two dotted lines depict the rate of potential decay for a monopole (top) and a dipole (bottom), respectively. The same presentation is used in most of the following figures. Note that in the original the curve is plotted for abscissa values $r/R < 26$, but we omitted data for $r/R > 12$ that have small ordinates and are difficult to accurately re-plot on a logarithmic scale.

Our re-analysis of these data shows that (i) EAP decay is consistent with an accelerating decay, and that (ii) there exists a critical distance, $r_0$, that forms a boundary between two regimes which differ in the multipole term that forms the best

approximation of the potential. At close ranges ( $r < r_0$ ), it is the monopole (exponent $k \approx 1$ ); and at intermediate ranges ( $r_0 < r < 12R$ ), it is the dipole (exponent $k \approx 2$ ). Examination of Figure suggests that $r_0 \approx 4R$ . Mean soma radius in pyramidal neurons in many cortical areas is $R \approx 9 \pm 2$ μm (see, e.g., [11-14]). Thus this early passive cable model predicts a dominant phenomenological dipole field for realistic cell-probe separations (i.e., $r > 35 \pm 10$ μm).

Rall's [1] model also predicts that the extracellular potential around the dendritic arbor will have approximate ("chunky") radial symmetry that makes polarity flips (or zero-crossings) virtually impossible to detect by an extracellular electrode.

## (2) Pettersen and Einevoll (2008) – a computational study

Pettersen and Einvoll [2] used analytic tools and also simulated passive cable models using realistic geometry of stellate and cat V1 layer 5 pyramidal neurons (the neurons modeled in [3]). For both cells, the monopole regime (decay with an exponent $k \approx 1$) was absent in the potential field at any $r > 20$ distances analyzed (the $r < 20$ μm range around the soma was excluded). A comparison with the results in [1] suggests that the branching and imperfect symmetry of the dendritic arbor in real neurons may be the key factors in significantly contracting the domain of the monopole.

For the pyramidal neuron, field decay was dipole-like ($k \approx 2$) at close range ($20 < r < 40$ μm), faster then dipole ($k \approx 2.5$), characteristic of a dominant mixture of dipole and quadrupole components, in the intermediate range ($60 < r < 200$ μm), and again dipole-like ($k \approx 2$) in the $500 < r < 1000$ μm range, as expected, for the quadrupolar contribution attenuates faster.

For the stellate neuron (which is a much smaller cell), field decay was dipole-like ($k \approx 2$) at close range ($20 < r < 40$ μm), dominated by the quadrupole component ($k \approx 3$) in the intermediate range ($60 < r < 100$ μm), and again dipole-like ($k \approx 2$) in the $100 < r < 200$ μm range. In comparison to the pyramidal cell, the higher degree of symmetry in the dendritic arbor in this cell allows the quadrupolar term to emerge as dominant in the intermediate range.

The Petersen and Einvoll [2] study concludes with the expectation "that the extracellular signature around real neurons will be dominated by a combination of dipolar and quadrupolar contributions; the highly symmetric arrangement of a ball-and-star model, which makes the octupole (exponent $k = 4$) the first nonzero multipole contribution, is unlikely to be seen for real cells."

The Petersen and Einvoll [2] study also showed that the dendritic arbor results in a low-pass spatial filtering, whose prominence increases with increasing temporal frequency; we will return to this in interpreting the Milstein and Koch [6] study below.

## (3) Moffitt and McIntyre (2005) – a computational study

Moffitt and McIntyre[4] simulated active cable models using realistic geometry of a cat V1 layer 5 pyramidal neuron (the neurons modeled in [3]), and analyzed EAP decay in directions both parallel and orthogonal to the apical dendrite. They plotted the results in their Figure 4 [4], which we re-analyze in Figure 2 below.

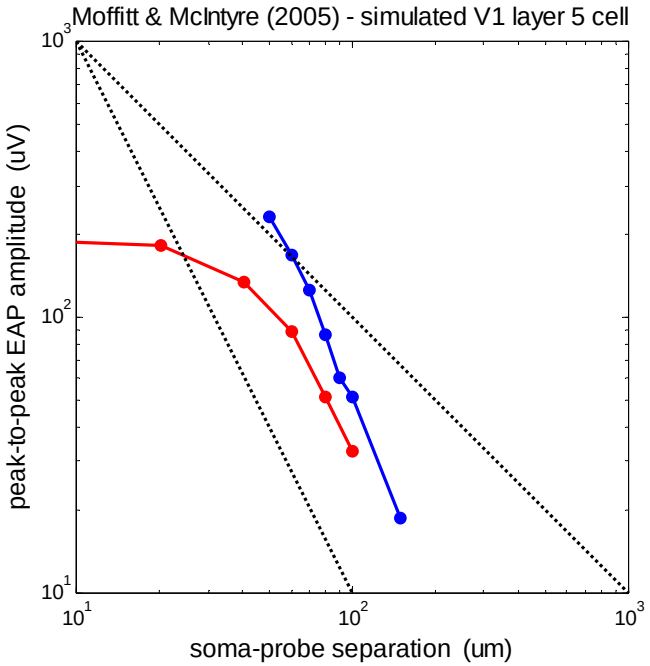


**Figure 2**

Data, re-plotted from Figure 4 in Moffitt and McIntyre[4], are results of realistic compartmental simulation of a reconstructed cat V1 layer 5 pyramidal neuron (same as in [3]). EAP amplitude was sampled along a line in two directions: in parallel to apical dendrite and 50 um away from soma (blue), and normal to apical dendrite at the soma level (red). Oblique lines depict the rate of potential decay for a monopole (top) and a dipole (bottom), respectively.

This active cable model predicts an accelerating spatial decay, starting out near the soma with a near constant potential. Within close range ($r < 40$ μm), spatial falloff is much slower than the monopole potential (exponent $k < 1$), but this quickly changes and in the distance range ($r > 50$ μm) the simulated potentials are consistent with a dipole-like field (exponent $k \approx 2$).

Note that the soma radius, $R$, is $\approx 10$ μm in cat V1 [14], thus Rall's $r_0 = 4R$ rule of thumb [1] predicts that the lower bound, $r_0$, on the radial range of the dipole regime is $\approx 40$ μm; Petersen and Einvoll's [2] estimate is smaller.

## (4) Lee et al (2007) – a computational study

Lee et al. [5] simulated a cat V1 layer 5 pyramidal (same as in [3]), and simulated a Thomas tetrode sampling the EAP in 3 positions, 50 μm apart. They used a monopole source model (exponent $k = 1$ ) to localize the cell soma from these samples. They summarized their results in their Fig. 1, which we re-plotted and re-analyzed in Figure 3A below.

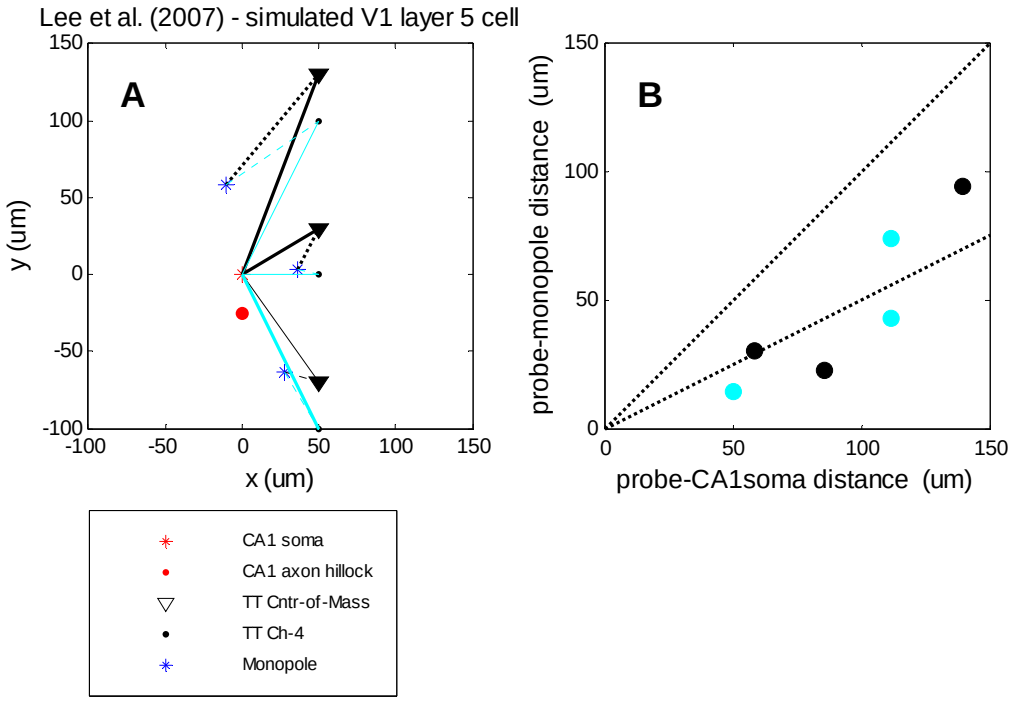


**Figure 3**

Data re-plotted from Figure 1 A-C Lee et al. [5]. (A) The 2D locations of the optimal monopole source model fitted to a simulated realistic V1 cell (soma at origin), whose EAP is sampled by tetrode in 3 recording positions. The V1 soma, axon hillock, the tetrode tip (at Ch-4), the center of mass of the 4 tetrode channels, and the optimal monopole model fitted to each tetrode position are indicated by symbols as in the legend. (B) Localization bias of monopole source model. The distance between the V1 soma and tetrode tip (filled circles) or center-of-mass of the 4 tetrode contacts (cyan circles) on the horizontal axis is plotted against the distances predicted by the optimal monopole model fitted to the 4 EAPs measured by the tetrode at each recording position. The top dashed line has slope of unity (corresponding to accurate localization; bottom one has slope of one half (corresponding to twofold underestimate by the monopole model, as expected for a true dipole source).

We also re-plotted Lee et al.'s results in terms of true cell-probe distance versus distance predicted by the monopole model (Figure 3B). The optimal monopole was located typically somewhere between the true soma position and the tetrode position: the true cell-probe distances sampled the $50< r <150$ μm range, but the monopole was localized, on average, at half the true distance. As shown in the Discussion, this is precisely the expected consequence of using a monopolar source model ($k = 1$) for a source whose spatial attenuation is dominated by a dipolar ($k = 2$) term: the distance bias is the ratio of the exponents.

As noted above for [4], Rall's rule of thumb [1] predicts that the lower bound, $r_0$, on the radial range of the dipole regime is $\approx 40$ μm in cat V1 pyramidal cells; Petersen and Einvoll's [2] estimate is smaller.

## (5) Milstein and Koch (2008) – a computational study

Milstein and Koch [6] simulated a realistic rat hippocampal CA1 pyramidal cell (the same as used in Gold et al. [8]), and derived the multipole expansion of the EAP field in the DC -limit. They find that, within the inner-field (roughly within one DC length constant, $\lambda_{DC} \approx 500\,\mu m$), no single multipole term dominates (their Figs 5-6). For $r < 120\ \mu m$ radial distances, the monopole term is largest; further out, between $200 < r < 500\,\mu m$, the dipole and quadrupole terms are comparable and larger than the other terms, and dipole is dominant beyond $r > 1000\ \mu m$.

To apply this study to the EAP's of spiking neurons, one must take into account the spatial filtering of the dendritic arbor, delineated by Pettersen and Einvoll [2]. That analysis showed that at the temporal frequencies characteristic of action potentials (~1000 Hz), effective length constants decrease due to the low-pass filtering of the dendritic arbor. The decrease is by a factor of 3-5 for dendrites of realistic length (200-to-1000 μm in cortical pyramidal cells). Thus, assuming an average attenuation factor 4 at those frequencies, the monopole term is expected to be largest in the $r < 30\ \mu m$ range; dipole and quadrupole terms to be comparable and largest in the $50 < r < 120\ \mu m$ range; and the dipole term emerges as dominant for $r > 250\ \mu m$. With the exception of the very nearest ($r < 30\ \mu m$) range of monopole dominance, these dipole and/or quadrupole regimes and their ranges are very comparable to those that were identified by Pettersen and Einvoll [2]. The correspondence is good despite the significant differences in the geometry and membrane properties of the cable models in the two studies: rat CA1 pyramidal cells and active membranes in Milstein and Koch [6] versus cat layer 5 pyramidal neurons (30-50% larger than in rat CA1) and passive membranes in Pettersen and Einvoll [2]. This similarity of results suggests that the key factor determining the intermediate-to-far dipole ranges is the shared model feature, the low-pass filtering by the passive dendritic arbor. Thus, for most realistic cell-probe separations ($r > 30\ \mu m$), the dipole, not the monopole, provides the best model approximation among the point multipole expansion terms used alone.

## (7) Gold et al. (2006) – a computational study

Using reconstructed dendritic morphology and active membrane conductances, Gold et al. [8] simulated realistic models of rat hippocampal CA1 pyramidal neurons (17 cells identified by Henze et al. [9]). The authors varied the active parameters to match the recorded waveform of the intracellular and extracellular action potentials (IAPs and EAPs) for each cell. For one cell they published simulation results that show the spatial dependence of the EAP amplitude in implicit form (their Figure 5A and B). Here we make explicit the EAP amplitude dependence on soma-probe separation in the direction perpendicular to the apical dendrite and plot it in Figure 4 below.

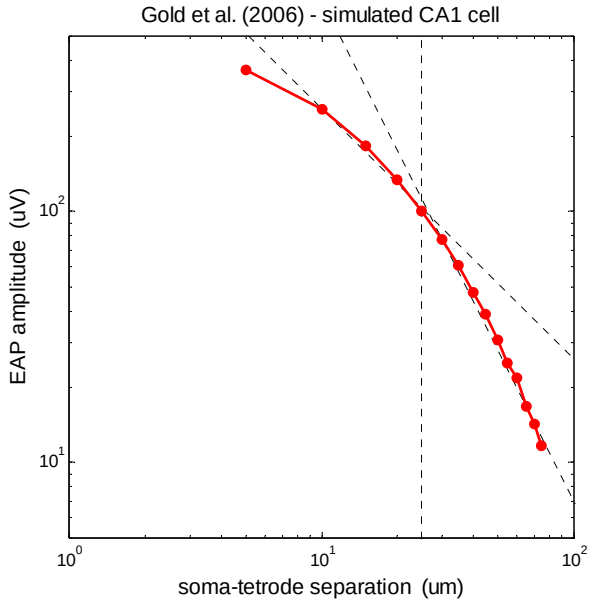


**Figure 4**

Data from Figure 5 A & B in Gold et al. [8] is re-plotted here (in red) in log-log coordinates. The plot shows the radial attenuation of the EAP amplitudes, sampled in a direction orthogonal to the apical densdrite, in a simulated realistic CA1 pyramidal cell model. Oblique lines tangent to the data depict the rate of potential decay for a pure monopole (left) and a dipole (right), respectively.

At the shortest ( $r < 25$ μm) range, radial potential attenuation follows an approximate monopole regime (exponent $k \approx 1$ ), but over the $30 < r < 75$ μm range the rate of attenuations rapidly increases to follow an approximate dipole regime ( $k \approx 2 \pm 0.5$ ).

Using slightly different active membrane conductances, the same authors ran a follow-up study [7] of the same neurons and report (their Figure 14.) an approximate monopolar fall-off (exponent on average, $k \approx 1.2$ ) of the EAP amplitudes over the more limited $0 < r < 50$ μm range from the soma (again in a direction orthogonal to apical dendrite).

Note that the soma radius, $R$ , is $\approx 8$ μm in rat CA1 [12, 13], thus Rall's $r_0 = 4R$ rule of thumb [1] predicts that the lower bound, $r_0$ , on the radial range of the dipole regime is $\approx 32$ μm.

## (8) Henze et al (2000) – an experimental study

Henze et al. [9] simultaneously recorded intracellular and extracellular action potentials (IAPs and EAPs) in rat hippocampal CA1 pyramidal cells. In these difficult dual recording experiments, they managed to record and localize 17 pyramidal cells that produced EAP amplitudes above the noise level (V>10 μV), and they show these EAP amplitudes as a function of soma-tetrode distance in their Figure 6. To analyze the radial attenuation in these data, we re-plotted them in log-log coordinates in our Figure 5 below.

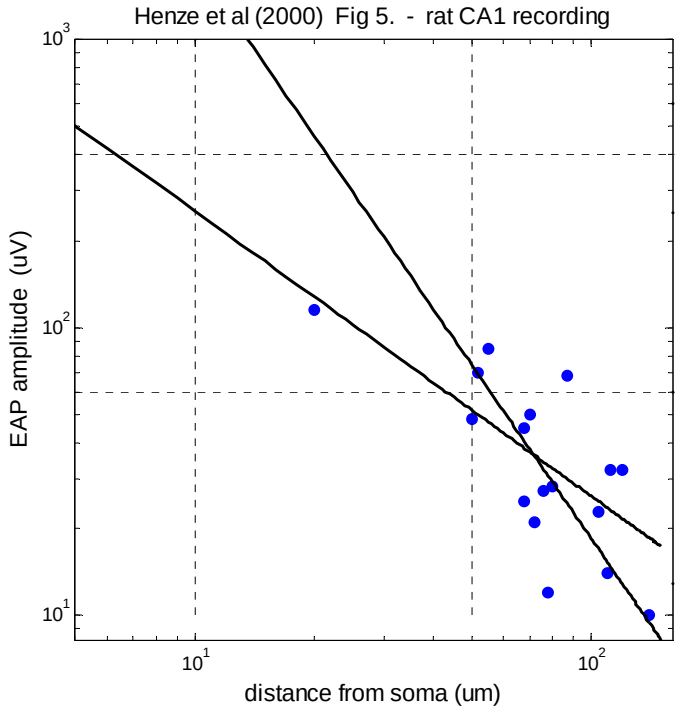


**Figure 5**

Data re-plotted (in blue) in log-log coordinates from Figure 6 of Henze et al.[9]. See text for more about the experiment. As guides to our analysis, we added these lines: EAP attenuation in the best fitting monopole (shallower oblique) and dipole (steeper oblique); average soma radius in CA1 (vertical line at ≈10 μm), tetrode recording radius (vertical line at ≈50 μm) estimated by authors at isolation threshold (horizontal line at ≈60 μV); and the largest EAP amplitudes (horizontal line ≈400 μV) recorded by authors (from their Figure 5.). Recording noise level was 10 μV.

The sample as a whole does not directly indicate the radial decay of EAP, because each neuron only contributes one data point (presumably because moving the tetrode

would destabilize the intracellular recording). Setting aside this concern, a power-law fit to these data is ambiguous: the data are consistent with the potential of both a monopole and a dipole field, depending on whether the fit includes the outlier at $r < 50\,\mu m$ ($k = 1.1 \pm 0.6$) or excludes it ($k = 1.3 \pm 0.9$). (The ± values are the 95%-confidence limits on the best fitting exponent.) These are not shown in our Figure 5 to avoid clutter, but both fits define lines that fall between the two oblique lines shown, the one on top indicating attenuation expected for a perfect monopole ($\sim r^{-1}$), and the one below for a dipole ($\sim r^{-2}$).

To find further experimental constraints on the exponent, we turn to the distribution of the EAP amplitude in a much larger CA1 sample (N=202) that was not probed intracellularly (Fig 5 in Henze et al.[9]). This sample spanned much larger potentials than the dually recorded sample (the range of peak-to-peak amplitudes was 100-600 μV; about 2/3 of this or about 60-400 μV is attributable to the negative peak amplitude – the measure used for the dually recorded sample). A dipole-like ($k \approx 2$) field decay can account the large EAP amplitudes without the need to modify other parameters, but the monopole requires distinctly larger current source size for the tetrode-only sample to avoid predicting physically unrealistic probe positions, i.e., a tetrode too close to or even virtually inside the soma. Although the introduction of the intracellular electrode is expected to interfere with the effective current source size (by creating a leak current and also altering the intracellular ionic concentration) and with the EAP spread (by the "shank" effect), the size and spatial dependence of the combined effect is unknown.

Note that the soma radius, $R$, is $\approx 8$ μm in rat CA1 [12, 13], thus Rall's $r_0 = 4R$ rule of thumb [1] predicts that the lower bound, $r_0$, on the radial range of the dipole regime is $\approx 32$ μm. The data of Henze et al.[9] is consistent with this lower bound.

In each example assessing EAP decay so far, distance was radial distance, i.e., measured from the soma. However EAP variation along a tangential direction can be very different from the $\sim r^{-2}$ even for a dipole. To highlight this point, we consider the EAP waveforms recorded by Henze et al.[9] with a silicon probe from 2 example neurons (a pyramidal cell and an interneuron) at multiple contact positions (their Figs 7-8), which

we re-plotted in Figure 6 below. The EAP decay assessed as a function of distance is well approximated by decay exponent $k \approx 1$. Note, though that in this analysis, the distance is *along the contact sites in the probe plane*, not radial distance from the neuron, and thus, it cannot be taken as evidence for a monopole-like field.

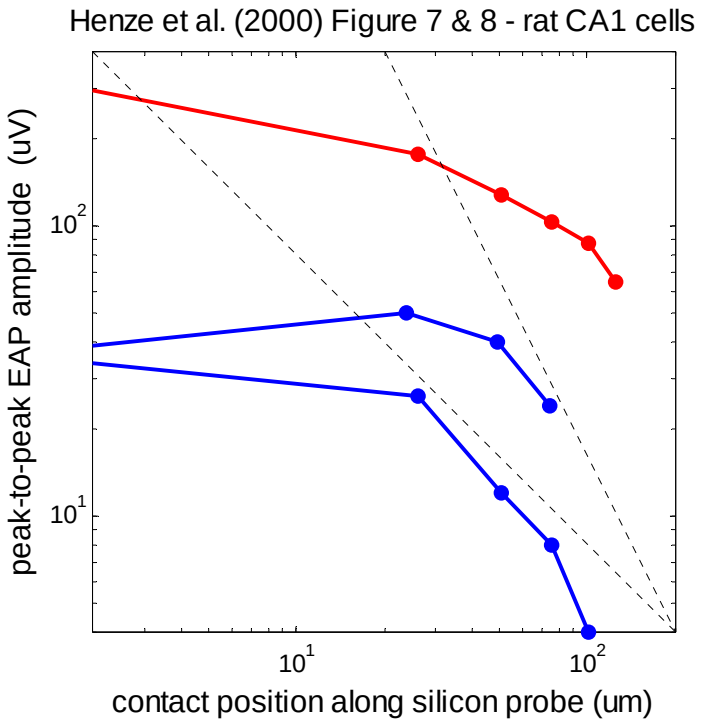


**Figure 6**

Rat CA1 data re-plotted in log-log coordinates from Henze et al.[9]. EAPs recorded by a linear silicon heptode (25-um contact spacing) from a pyramidal cell (in blue, from their Figure 7), and an interneuron (in red, from their Figure 8). Oblique lines indicate radial (not tangential) EAP decay for a monopole (shallower) and a dipole (steeper).

## (9) Cohen and Miles (2000) – an experimental study

Cohen and Miles [10] recorded intracellular and extracellular action potentials (IAPs and EAPs) in CA3 pyramidal cells in *in vitro* slices (guinea pig hippocampus). Their extracellular probe was a single electrode (and the intracellular electrode was a sharp electrode, as in [9]). Peak-to-peak EAP amplitudes, recorded in 10 pyramidal neurons (each at 2 distances), were pooled in 4 bins of distances and separately averaged to produce the plot of radial EAP attenuation in their Figure 2C that we re-plotted in the familiar log-log coordinates in Figure 7 below. The data are consistent with an accelerating EAP attenuation: it is slower than monopolar at radial distances $r < 50$ µm, and approximately dipolar for $r > 50$ µm. Note that the soma radius, $R$, is $\approx 9$ µm in guinea pig CA3 [10], thus Rall's $r_0 = 4R$ rule of thumb [1] predicts that the lower bound, $r_0$, on the radial range of the dipole regime is $\approx 35$ µm.

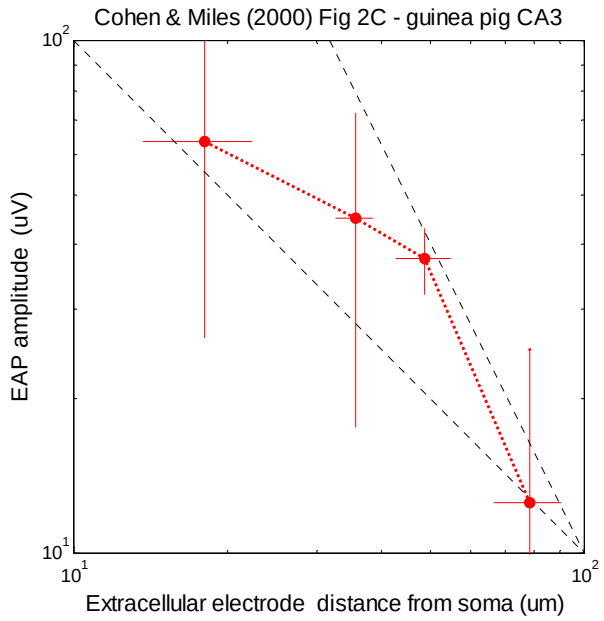


**Figure 7** Data, re-plotted (in red) in log-log coordinates from Fig. 2C of Cohen and Miles [10], represent recordings from 10 pyramidal neurons (each contributing to 2 distances, a total 20 measurements). The averages at 4 successive distances result from pooling 5, 6, 4, and 5 measurements, respectively (the authors gave no further detail of binning and averaging). We added the 2 oblique lines to indicate the rate of radial EAP decay expected for a monopole (shallower) and a dipole (steeper). Recording noise level was ~10 µV.

## References


1. Rall, W., *Electrophysiology of a dendritic neuron model.* Biophys J, 1962. **2**(2 Pt 2): p. 145-67.
2. Pettersen, K.H. and G.T. Einevoll, *Amplitude variability and extracellular low-pass filtering of neuronal spikes.* Biophys J, 2008. **94**(3): p. 784-802.
3. Mainen, Z.F. and T.J. Sejnowski, *Influence of dendritic structure on firing pattern in model neocortical neurons.* Nature, 1996. **382**(6589): p. 363-6.
4. Moffitt, M.A. and C.C. McIntyre, *Model-based analysis of cortical recording with silicon microelectrodes.* Clin Neurophysiol, 2005. **116**(9): p. 2240-50.
5. Lee, C.W., H. Dang, and Z. Nenadic, *An efficient algorithm for current source localization with tetrodes.* Conf Proc IEEE Eng Med Biol Soc, 2007. **2007**: p. 1282-1285.
6. Milstein, J.N. and C. Koch, *Dynamic Moment Analysis of the Extracellular Electric Field of a Biologically Realistic Spiking Neuron.* Neural Computation, 2008. **20**(8): p. 2070-2084.
7. Gold, C., D.A. Henze, and C. Koch, *Using extracellular action potential recordings to constrain compartmental models.* J Comput Neurosci, 2007. **23**(1): p. 39-58.
8. Gold, C., et al., *On the origin of the extracellular action potential waveform: A modeling study.* J Neurophysiol, 2006. **95**(5): p. 3113-28.
9. Henze, D.A., et al., *Intracellular features predicted by extracellular recordings in the hippocampus in vivo.* J Neurophysiol, 2000. **84**(1): p. 390-400.
10. Cohen, I. and R. Miles, *Contributions of intrinsic and synaptic activities to the generation of neuronal discharges in in vitro hippocampus.* J Physiol, 2000. **524 Pt 2**: p. 485-502.
11. Larkman, A. and A. Mason, *Correlations between morphology and electrophysiology of pyramidal neurons in slices of rat visual cortex. I. Establishment of cell classes.* J Neurosci, 1990. **10**(5): p. 1407-14.
12. Altemus, K.L., et al., *Morphological characteristics and electrophysiological properties of CA1 pyramidal neurons in macaque monkeys.* Neuroscience, 2005. **136**(3): p. 741-756.
13. Ishizuka, N., W.M. Cowan, and D.G. Amaral, *A quantitative analysis of the dendritic organization of pyramidal cells in the rat hippocampus.* The Journal of Comparative Neurology, 1995. **362**(1): p. 17-45.
14. Sholl, D.A., *Dendritic organization in the neurons of the visual and motor cortices of the cat.* J Anat, 1953. **87**(4): p. 387-406.